

# Paramagnetic Meissner, vortex and 'onion' ground states in Fulde-Ferrell finite-size superconductor

V. D. Plastovets<sup>1,2,3,\*</sup> and D. Yu. Vodolazov<sup>1,†</sup>

<sup>1</sup>*Institute for Physics of Microstructures, Russian Academy of Sciences, 603950, Nizhny Novgorod, GSP-105, Russia*

<sup>2</sup>*Lobachevsky State University of Nizhny Novgorod, Nizhny Novgorod, 603950 Russia*

<sup>3</sup>*Sirius University of Science and Technology, 1 Olympic Ave, 354340 Sochi, Russia*

(Dated: September 25, 2021)

We theoretically find that finite size Fulde-Ferrell (FF) superconductor (which is characterized by spatially nonuniform ground state  $\Psi \sim \exp(-i\mathbf{q}_{FF}\mathbf{r})$  and  $|\Psi|(r) = \text{const}$  in the bulk case, where  $\Psi$  is a superconducting order parameter) has paramagnetic Meissner, vortex and 'onion' ground states with  $|\Psi|(r) \neq \text{const}$ . These states are realized due to boundary effect when the lateral size of superconductor  $L \sim 1/q_{FF}$ . We argue, that predicted states could be observed in thin disk/square made of superconductor-ferromagnet-normal metal trilayer with  $L \simeq 150 - 600\text{nm}$ .

PACS numbers:

## I. INTRODUCTION

Majority of superconductors expel weak enough external magnetic field which means that they are diamagnets. Mathematically this property of superconductor can be described via London relation between vector potential  $\mathbf{A}$  and superconducting current density  $\mathbf{j}_s$ :

$$\mathbf{j}_s = -\frac{c}{4\pi\lambda^2}\mathbf{A}, \quad (1)$$

where  $\lambda$  is the London penetration depth which determines how deep magnetic field penetrates the superconductor. However in special case of so-called odd-frequency superconductivity<sup>1-7</sup> the sign in Eq. (1) may be opposite which corresponds to paramagnetic response and formally negative density of Cooper pairs  $n \sim \lambda^{-2} < 0$ . Such a paramagnetic response can be realized locally in different superconducting systems with spatially nonuniform superconducting order parameter: ferromagnetic (F) layer coupled to s-wave superconductor (S)<sup>1,6,7</sup> (as a practical realization it could be ferromagnet/normal metal bilayer coupled with s-wave superconductor<sup>8</sup>); normal metal (N) layer coupled to p-wave superconductor<sup>2</sup> or to s-wave superconductor with spin-active SN interface<sup>3</sup>; nonequilibrium N layer coupled to s-wave superconductor<sup>9,10</sup>; near the edge of clean p- or d-wave superconductor<sup>4,11</sup>.

If thickness of the superconductor in hybrid SF or SN bilayers is small the paramagnetic response of proximity induced odd-frequency superconductivity in F or N layer may exceed the diamagnetic response of the host superconductor which leads to global paramagnetism. It may signal about instability and appearance of modulated, along hybrid structure, Fulde-Ferrell-Larkin-Ovchinnikov (FFLO) like superconducting state<sup>12,13</sup> which has zero magnetic response ( $\lambda^{-2} \rightarrow 0$  in Eq. [1]). In Larkin-Ovchinnikov state the modulated state corresponds to the standing wave (superconducting order parameter  $\Psi \sim \cos(\mathbf{q}_{LO}\mathbf{r})$ ) while in Fulde-Ferrell state  $\Psi \sim \exp(i\mathbf{q}_{FF}\mathbf{r})$ . Note that in the FF state spontaneous currents can flow in the ground state<sup>13,14</sup> which are absent

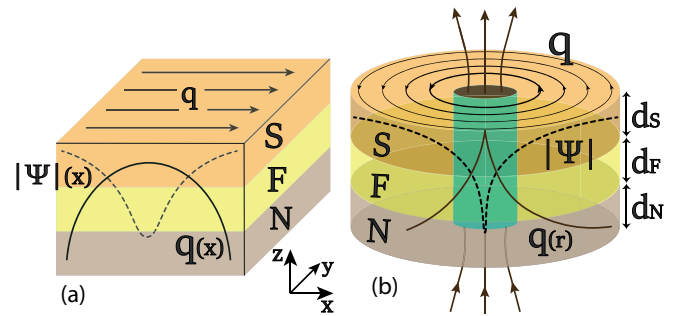


FIG. 1: (a) Superconductor-ferromagnet-normal metal superconducting square being in quasi 1D Fulde-Ferrell state and (b) SFN disk being in vortex state. Dashed and solid curves correspond to distribution of  $|\Psi|$  (the superconducting order parameter, averaged over the thickness) and  $q$  ( $\sim$  supervelocity), respectively.

in LO state.

In our work we theoretically study how ground state of FF superconductor is modified when its lateral size becomes about of  $1/q_{FF}$ . As a practical realization we have in mind square/disk made of trilayer superconductor/ferromagnet/normal metal (see Fig. 1) where FF state can exist<sup>14</sup>. We do not consider LO state because in Ref.<sup>15</sup> it has been found that in SFN trilayer FF state has lower energy than LO one. Due to vanishing of normal component of superconducting current  $j_s$  at the border with vacuum in each (S, F and N) layer one has to have  $q = (\nabla\phi + 2\pi A/\Phi_0)|_n = 0$  ( $\phi$  is the phase of superconducting order parameter) which should affect the classical Fulde-Ferrell (plain wave) state. In Refs.<sup>16,17</sup> it was found, that such a modification occurs on scale about of  $1/q_{FF}$  and it leads to increase of the free energy  $F$ . Therefore when  $Lq_{FF} \sim 1$  this increase of free energy may exceed the energy gain from transition to modulated state and homogenous state becomes more favorable. Support to this comes from Ref.<sup>18</sup> where it was found that FFLO disk with radius  $Rq_{FF} \lesssim 1.2$  has higher critical temperature in homogenous state than in

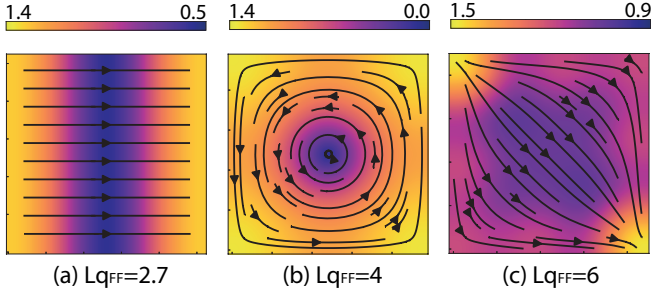


FIG. 2: Distribution of the dimensionless superconducting order parameter  $|\Psi|(x, y)$  and of  $\mathbf{q}(x, y)$  (black arrows) in FF square with different lateral size  $L$ . For all cases, the ground states are shown (for  $Lq_{FF} < \pi/\sqrt{2}$  ground state is the homogenous state with  $q = 0$  - not shown here). (a) quasi 1D FF like state with  $\mathbf{q} = (q(x), 0)$ , (b) the single vortex state, (c) the FF like state with  $\mathbf{q} = (q_1(x, y), q_2(x, y))$ . The ground states are degenerate - the energy is not changed with reversal of  $\mathbf{q}$ .

FFLO one.

Our main result can be formulated as follows. We find that when  $Lq_{FF} \lesssim 2$  the ground state of FF superconductor is spatially homogenous with  $q = 0$  and it has global paramagnetic response ( $\lambda^{-2} < 0$ ) at small enough magnetic fields. With increasing  $L$  there is a second-order transition to quasi 1D state with  $\lambda^{-2} = 0$  (see Fig. 1(a) or Fig. 2(a)) which becomes energetically less favorable than single vortex state with spatially dependent  $\lambda^{-2}$  and  $|\Psi|$  (see Fig. 1(b) or Fig. 2(b)) at larger  $L$ . With further increasing  $L$  the 'onion' like state (see Fig. 2(c)) has the lowest energy.

In our calculations we use two models. Numerical solution of Usadel equation for 3D square shown in Fig. 1 is rather complicated and time-consuming problem. Therefore we use 2D modified phenomenological Ginzburg-Landau (GL) equation (see appendix A) for *thickness averaged* superconducting order parameter  $\Psi$  which qualitatively well describes main properties of FF superconductor<sup>16,17,19</sup> and allows us to find arbitrary in-plane distribution of  $\Psi$ ,  $\lambda^{-2}$  and sheet current density. Besides we use 2D Usadel equation (with radial and  $z$  dependence) for SFN disk where we consider only circularly symmetric (vortex) and spatially homogenous states. The last approach allows us to confirm results found from GL model and determine appropriate material parameters for the experimental verification of the predicted results.

## II. GINZBURG-LANDAU APPROACH

First we present our results found from solution of modified 2D Ginzburg-Landau equation (equation, boundary conditions, parameters and numerical method are presented in appendix A). In Fig. 2 we show distribution of the superconducting order parameter  $|\Psi|$  and  $q$

in FF superconducting square being in different ground states. For  $Lq_{FF} \leq \pi/\sqrt{2}$  the ground state corresponds to spatially homogenous state ( $q = 0$ ) with  $\lambda^{-2} < 0$ . In narrow range  $\pi/\sqrt{2} \leq Lq_{FF} \lesssim 2.5$  the quasi 1D Fulde-Ferrell like state with  $\lambda^{-2} = 0$ , has the smallest energy (see Fig. 2(a)), while for  $2.5 \lesssim Lq_{FF} \lesssim 4.6$  the vortex state is a ground one (see Fig. 2(b)) with  $\lambda^{-2}(x, y) < 0$  (see Fig. 3a). For  $Lq_{FF} \gtrsim 4.6$  the state with spatial distribution of  $|\Psi|$  and  $q$  resembling the onion is realized (Fig. 2(c)). In 'onion' state the diagonal distribution of  $q$  minimizes the positive contribution to the free energy which comes from vanishing of  $q|_n$  at the edge<sup>17</sup>. In homogenous and quasi-1D FF states the current density is equal to zero, while in the vortex and 'onion' states it is finite (see Fig. 3).

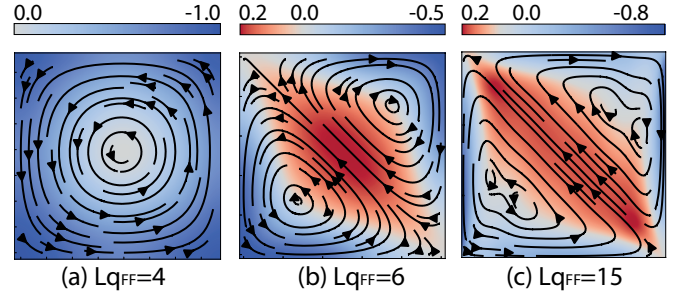


FIG. 3: Spatial distribution of local  $\lambda^{-2}$  and superconducting current density (arrows) in squares being in vortex (a) and 'onion' (b, c) states. Red color corresponds to  $\lambda^{-2} > 0$  (diamagnetic response), blue one -  $\lambda^{-2} < 0$  (paramagnetic response). One can see that in 'onion' state there are eddy currents, but vorticity  $N = \oint \nabla \phi d\mathbf{l} / 2\pi$  is equal to zero. This result resembles the eddy currents in d- and p-wave mesoscopic disks<sup>11</sup> with the only qualitative difference that in 'onion' state eddy currents are finite even at zero magnetic field.

In FF square various metastable states may exist and their number increases with increasing of  $L$  as in ordinary mesoscopic superconductor (see for example<sup>21</sup>). In Fig. 4 we show examples of such states. These are vortex free state (not the 'onion' one - compare Fig. 4(a) and Fig. 2(c)) and states with different number of vortices, including the states with vortices and antivortices (Figs. 4(e, f)). In ordinary finite-size (sometimes it is also called mesoscopic) superconductor vortex states are stable in presence of the magnetic field  $H$  (including vortex-antivortex molecule<sup>22,23</sup>), while in FF superconductor they are stable even at  $H = 0$ . Their stability comes from decreasing of the free energy and increase of  $|\Psi|$  in presence of finite  $q$  (which is proportional to super-velocity). In contrast, in ordinary superconductor finite  $q$  leads to increase of  $F$  and suppression of superconductivity. The metastable and ground states are degenerative - their energy does not change with reversal of  $q$  and/or change the position of vortices. For instance, in case of state shown in Fig. 4(b) there are three more states with the same energy that can be realized by placing the vor-

tex in different quarters of the square.

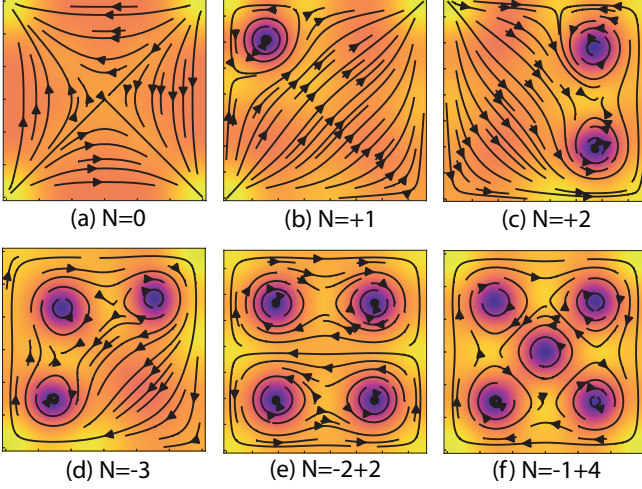


FIG. 4: Distribution of magnitude of the superconducting order parameter  $|\Psi|(x, y)$  (colormap) and  $\mathbf{q}(x, y)$  (black arrows) in square with  $Lq_{FF} = 8$ , being in various metastable states.  $N$  is a total vorticity ( $N = \oint \nabla \varphi d\mathbf{l} / \sqrt{2\pi}$ , the contour  $\mathbf{l}$  is positively oriented along the boundaries).

In Fig. 5 we show dependence of the free energy  $F$  and magnetic moment  $M = -dF/dH$  of FF square with the different  $L$  on the magnetic field. Homogenous and 1D states demonstrate paramagnetic response at low fields (see Fig. 5(a,b)) which transforms to diamagnetic one at large fields. Because free energy decreases at low fields one can expect magnetic field induced enhancement of critical temperature. Similar field induced enhancement of  $T_c$  was predicted for bulk FFLO superconducting film being in parallel magnetic field<sup>10,15</sup>, FFLO disk of small radius<sup>18</sup> and 1D superconducting FFLO ring<sup>24</sup> being in perpendicular magnetic field. Due to small size of the square it cannot accommodate vortex even near critical magnetic field which is also typical for ordinary small-size superconductor. Because of that dependence  $M(H)$  is not hysteretic.

Vortex (Fig. 5(c)) and 'onion' (Fig. 5(d)) states have more complicated  $M(H)$  dependence because of entry/exit of vortices and antivortices. In Fig. 5(c) we show evolution of magnetic moment with increasing and decreasing of  $H$  for square being initially in vortex state. Perpendicular small magnetic field decreases  $q$  in the square and it results to increase of free energy and diamagnetic response. At  $H \sim 0.4H_{GL}$  vortex exits and antivortex enters, which considerably lowers the free energy and leads to the change of sign of  $M$ . It is interesting, that at  $H \sim 1.5H_{GL}$  antivortex exits and square goes to Meissner (vortex free) state which has the lowest energy in some range of magnetic fields among other states. It happens due to absence of the vortex core which increases the free energy while supervelocity is large enough due to the magnetic field. At  $H \sim 2.5H_{GL}$  the Meissner state becomes unstable and vortex enters the square. At

$H \sim 3.2H_{GL}$  square goes to normal state. With decreasing of magnetic field the square passes through vortex, Meissner and finally, antivortex states. The dependence  $M(H)$  is hysteretic, as in case of ordinary mesoscopic superconductor, due to presence of energy barriers for vortex/antivortex entry/exit. Note, that in such a square one also can expect field enhanced critical temperature because free energy is lower at finite magnetic field than at  $H = 0$ .

Evolution of magnetic properties of the square being in 'onion' ground state at  $H = 0$  is more complex (see Fig. 5(d)). At  $H \sim 0.15H_{GL}$  there is first order transition from 'onion' to another vortex free state where magnetic response is paramagnetic (at lower fields magnetic response is weak and diamagnetic). At  $H \sim 0.25H_{GL}$  there is a transition to antivortex state with  $N=-1$  and then antivortex is replaced by a vortex ( $N=1$ ) at  $H \sim H_{GL}$ . The number of vortices is growing with increasing  $H$  to  $N=8$  and, finally, square goes into the normal state.

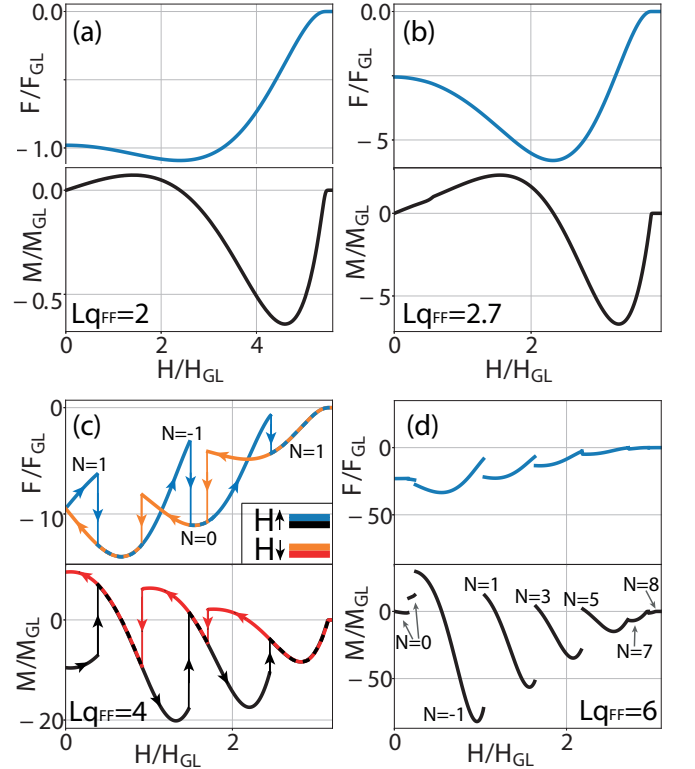


FIG. 5: Magnetic field dependence of the free energy and magnetic moment of FF squares with different lateral size shown in figures. In figures (a,b)  $M(H)$  is reversible (no vortices at any  $H$ ), while in figures (c,d) it is hysteretic (in (d) we show  $M(H)$  only in increasing magnetic field).  $N$  is the vorticity (number of vortices). Free energy is scaled in units of  $F_{GL}$  (see Appendix A), magnetic field is in units of  $H_{GL} = \Phi_0 / 2\pi\xi_{GL}^2$  and magnetic moment is in units of  $M_{GL} = F_{GL} / H_{GL}$ .



### III. USADEL APPROACH

Our calculations in framework of microscopic Usadel approach for SFN disk supports some results found in GL model (for details of the method see Appendix B). We consider only circularly symmetric states (homogenous and vortex ones) because finding of states similar to ones shown in Fig. 2(a,c) and Fig. 4 needs solution of 3D Usadel equation, together with finding  $q(\vec{r})$ . In Fig. 6 we show difference between free energies of homogenous and vortex states as a function of radius of the SFN disk. Free energy (per unit of square) is normalized in units of  $F_0 = \pi N(0)(k_B T_{c0})^2 \xi_c$ , where  $\xi_c = (\hbar D_S / k_B T_{c0})^{1/2}$ ,  $N(0)$  is a one spin density of states in superconductor,  $T_{c0}$  is a critical temperature of single S layer and  $D_S$  is its diffusion coefficient. One can see that starting from some radius  $R_c$  (its value depends on temperature) vortex state becomes energetically more favorable than homogenous one. Taking into account that in bulk FF state  $q_{FF} \simeq 0.16/\xi_c$  at  $T = 0.1T_{c0}$  (see Fig. B.1) we estimate  $2R_c \simeq 20\xi_c \simeq 3.2/q_{FF}$  (for  $T = 0.3T_{c0}$  we have  $2R_c \simeq 38\xi_c \simeq 4.5/q_{FF}$ ) which is close to the numerical value, obtained with help of modified GL equation for the square and to the analytical result  $2R_c \simeq 2.4/q_{FF}$  found from linearized GL equation for the disk near  $T_c$  (see Fig. 2 in<sup>18</sup>). From Fig. 6 it also follows that there exists temperature driven first order transition from homogenous to vortex state as one decreases temperature.

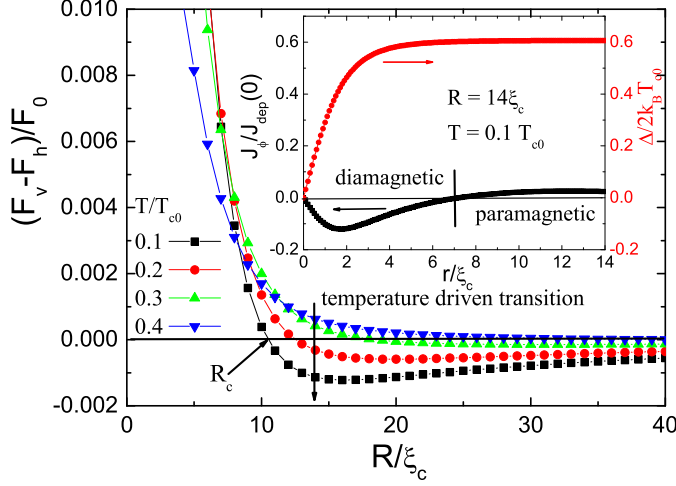


FIG. 6: Dependence of the difference between free energies of the homogenous ( $F_h$ ) and single vortex ( $F_v$ ) states on radius of SFN disk. In inset we show the radial dependence of sheet current density and magnitude of superconducting order parameter in Usadel model  $\Delta$  in S layer on the boundary with vacuum. Parameters of SFN disk:  $d_S = 1.4\xi_c$ ,  $d_F = 0.15\xi_c$ ,  $d_N = \xi_c$ , exchange energy in F layer is  $E_{ex} = 25k_B T_{c0}$ .

In the vortex ground state there is a finite sheet current  $J = \int j_s dz$  - see inset in Fig. 6. In contrast to the vortex in ordinary superconductor the sheet current

density changes sign across the disk because in different parts of the trilayer  $\int \lambda^{-2} dz$  has different sign. Note that in framework of GL model one has  $\int \lambda^{-2} dz < 0$  in the vortex state everywhere in the FF square and there is no sign change of  $J$  (see Fig. 3(a)). In SFN structure the size of the vortex core is different in S (where it is about of  $\xi_c$ ) and N (where it is about of  $\xi_N = (\hbar D_N / k_B T)^{1/2} \gg \xi_c$ ) layers. This difference has been observed recently in SN bilayer<sup>28,32</sup>. Due to vanishing of superconducting order parameter in the center of vortex core the proximity induced odd-frequency superconductivity is suppressed in N layer on scale about of  $\xi_N$  around the vortex core and it leads to  $\lambda^{-2} > 0$  there. Apparently this effect is not caught by used phenomenological GL model.

Vortex state is a double degenerative state because states with opposite vorticity have the same energy (if one neglects interaction of vortex induced magnetic field with ferromagnet layer). Using typical parameters of NbN as a S layer (resistivity  $\rho_n = 200\mu\Omega \cdot \text{cm}$ , diffusion coefficient  $D = 0.5\text{cm}^2/\text{s}$ ,  $T_{c0} = 10\text{K}$ ,  $\xi_c = 6.4\text{nm}$ ) and other parameters as in Fig. 6 we find magnetic field in the center of vortex  $\sim 2\text{Oe}$  ( $R = 14\xi_c$ ). This magnetic field is much smaller than thermodynamic field of NbN:  $H_c = \sqrt{4\pi N(0)(1.76k_B T_{c0})^2} \sim 10^3\text{Oe}$  and it gives small contribution to the free energy (smaller than  $10^{-4}F_0$ ). Besides this field is too small to affect magnetic properties of F layer but it is large enough to be measured by SQUID magnetometer (especially if there is an array of SFN disks).

We also find that energy of the giant vortex state with vorticity  $N \geq 2$  is larger than single vortex state when  $R < 40\xi_c$  due to larger vortex core. We do not consider larger disks because we expect that 'onion' state is more energetically favorable in such samples.

Making a hole in the center of SFN disk favors appearance of vortex state because there is no positive contribution from the vortex core to the free energy. For example for SFN ring with parameters as in Fig. 6 and width  $\xi_c$  the homogenous state becomes unfavorable at  $R \gtrsim 5\xi_c$ . For smaller rings supervelocity  $v_s \sim q \sim 1/R$  is too large and homogenous state has smaller energy.

In Fig. 7 we show calculated field dependencies of free energy and magnetic moment of SFN disks with different radii being either in vortex or Meissner states. In contrast to GL approach we cannot determine at which magnetic fields vortex/antivortex/Meissner states become unstable in the used model. Nevertheless these results support some conclusions following from GL model. Namely, disk being in homogenous (Meissner) state has paramagnetic response up to some magnetic field where it changes to ordinary diamagnetic one (compare with Fig. 5(a,b)). It occurs roughly at  $H \sim H^* \simeq \Phi_0/\xi_N R$  ( $\xi_N = \sqrt{\hbar D_N / k_B T}$ ) when proximity induced superconductivity in N layer is got suppressed.

Evolution of states in SFN disk where vortex state is ground one at  $H = 0$  (see Fig. 7 for disk with  $R = 14\xi_c$ ) qualitatively resembles results found in GL model. Free energy increases at small fields and there is range of the

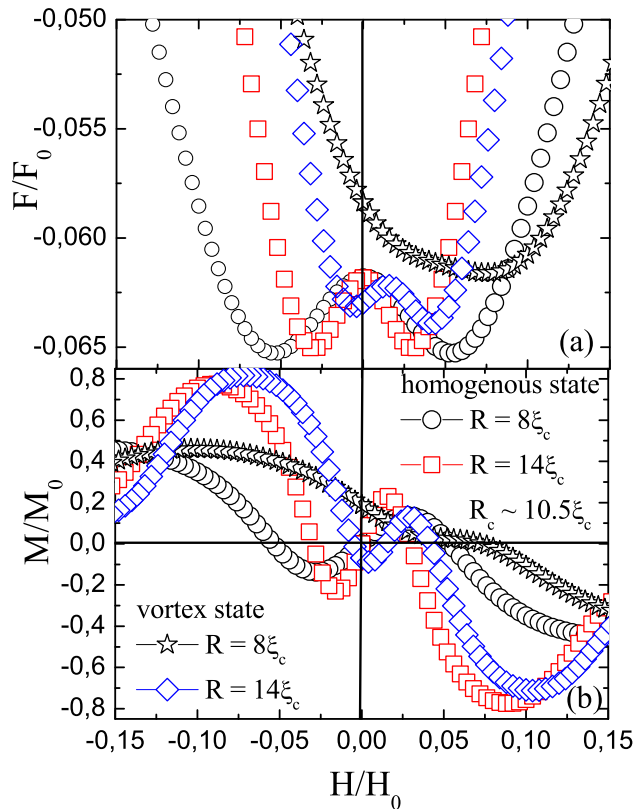


FIG. 7: (a) Dependence of the free energy of SFN disks being in homogenous and vortex states on magnetic field ( $H_0 = \Phi_0/2\pi\xi_c^2 \sim 7.8T$  for NbN). (b) Dependence of the magnetic moment (measured in units of  $M_0 = 2\pi\xi_c^2 R^2 j_{dep}(0)/c$ ) of SFN disks on the magnetic field. Parameters of the disks as in Fig. 6.

fields where the Meissner state has the lowest energy while at large fields vortex state becomes again more favorable. From Fig. 7 one may also conclude that antivortex state (it corresponds to vortex in negative magnetic field in Fig. 7) decreases its energy at small  $|H|$  which also coincides with our findings in GL model. Unusual behavior changes on conventional one at  $H > H^*$  when proximity induced superconductivity dies in N layer.

Smaller size disk ( $R = 8\xi_c$ ) with vortex demonstrates different behavior at low fields, but it is not clear if vortex state is stable there. We are only sure that at large fields ( $H > H^*$ ), vortex state is more favorable than Meissner one as in ordinary superconductors.

The similar results could be found for different material parameters of SFN disk. For example one can take F layer with larger or smaller exchange energy - it leads only to different needed thickness of F layer when FF state could be realized (see Fig. S4 in<sup>14</sup>). One also may increase thickness of N layer - it shifts the temperature where bulk FF state appears (see Fig. S3(a) in<sup>14</sup>). More

crucial influence on the predicted effect comes from increasing of  $d_S$ . While the bulk FF state could be realized in case of relatively thick  $d_S \gtrsim 3\xi_c$  (see Fig. S3(b) in<sup>14</sup>) the energy gain of bulk FF state in comparison with homogenous state decreases with increasing  $d_S$ , as well as  $|\lambda^{-2}| \rightarrow 0$  in homogenous state. As a result difference in energy between all considered ground states decreases too and some of them could disappear. For example in the vortex state large positive contribution to  $F$  comes from the vortex core and it could exceed the negative contribution to  $F$  due to finite  $q$  around the vortex.

#### IV. DISCUSSION

In contrast to other systems where *global* 'paramagnetic Meissner effect' (PME) was theoretically or experimentally found (high  $T_c$  materials<sup>4</sup>, superconductors with bulk pinning<sup>25,26</sup> or ordinary mesoscopic superconductors<sup>27</sup>) in FF finite-size superconductor it exists in the ground state when there is no any frozen magnetic flux (trapped vortices). In this sense similar global PME was also predicted for unconventional (p or d-wave) superconducting disk where it may exist due to edge paramagnetic currents<sup>11</sup>.

Ground and metastable states in SFN disk/square could be observed with help of scanning tunnelling spectroscopy. In recent paper<sup>28</sup> SN nanostructure (MoGe/Au) with needed geometrical and physical parameters was studied. Indeed, Au is a pure metal with residual resistance  $\rho_N \simeq 2\mu\Omega \cdot \text{cm}$  even for 20 nm thick film<sup>29</sup>, while MoGe is rather dirty metal with  $\rho_S \simeq 180\mu\Omega \cdot \text{cm}$ ,  $T_{c0} = 6.5K$  and  $D \simeq 0.4\text{cm}^2/\text{s}$ <sup>30</sup> ( $\xi_c \simeq 6.8\text{nm}$ ). To observe predicted states one needs to add ferromagnet layer, made from CuNi, for example, with thickness  $d_F \sim 2 - 3\text{nm}$  (it should be equal approximately to half of thickness of ferromagnet in NbN/CuNi/NbN trilayer where  $\pi$  Josephson junction has been recently realized<sup>31</sup>). In homogenous state superconducting order parameter is homogenous while in quasi 1D, vortex and 'onion' states it depends on coordinate due to  $q(x, y)$  (see Fig. 2). We also have to add, that spatial variation of local density of states (LDOS) is rather different in S and N layers due to different length scales ( $\sim \xi_c$  in S layer and  $\sim \xi_N$  in N layer) leading, for example, to rather different size of vortex core in S and N layers<sup>28,32</sup> and this circumstance should be taken into account in the experiment.

From our calculations made in framework of Usadel model and parameters of NbN or MoN it follows that lateral size of the square/disk should be less than  $20\xi_c \simeq 130\text{nm}$  (see Fig. 6) to observe paramagnetic Meissner state. Vortex state exists in slightly larger squares/disks while 'onion' state could be observed in samples with lateral size as large as 600 nm as it follows from modified GL model (see Fig. 1(c) in<sup>20</sup> and for estimation we take  $1/q_{FF} \sim 6\xi_c$ ).

Depending on the parameters the FF phase may exist

at  $T < T_c^{FFLO} = T_c$  or at  $T < T_c^{FFLO} < T_c$ <sup>14</sup>. In first case  $1/q_{FF}$  is finite at  $T = T_c$  and, hence, at  $T < T_c$  the homogenous paramagnetic state may exist only in superconductor of small size with  $Lq_{FF} \lesssim 2-3$ . In the second case one can expect transition from the paramagnetic to quasi 1D state shown in Fig. 2(a) (because it is second-order transition), as one decreases temperature below  $T_c^{FFLO}$  ( $1/q_{FF}$  decreases from infinity at  $T = T_c^{FFLO}$  up to finite value at lower temperature) but it may happen that for transition to vortex or 'onion' state one needs to overcome the energy barrier. If the energy barrier is too high the superconducting square will stay in quasi 1D state. In this case one can use perpendicular magnetic field to switch Fulde-Ferrell superconductor from one state to another one, as it is demonstrated in section II.

We expect small influence of edge or bulk defects on our results due to large  $\xi_N \gg \xi_c$ . For considered above N layers  $\xi_N > 50$  nm which is comparable with the size of SFN disk or square where these states could be observed.

## V. SUMMARY

We find that Fulde-Ferrell finite size superconductor may have different ground states. Depending on the lateral size it could be either in homogenous paramagnetic state, quasi 1D, vortex or 'onion' states. We propose that these states could be realized in square(disk) made of superconductor/ferromagnet/normal metal trilayer with lateral size 150-600 nm, where superconductor is dirty superconducting material (like NbN, MoGe, NbTiN and so on), normal metal is Au, Ag, Al or Cu and ferromagnet is CuNi or other weak ferromagnetic material.

## Acknowledgments

Authors acknowledge support from Foundation for the Advancement of Theoretical Physics and Mathematics "Basis" (grant 18-1-2-64-2) and Russian Foundation for Basic Research (project number 19-31-51019).

## Appendix A: Modified Ginzburg-Landau model

The modified Ginzburg-Landau free energy functional describing 2D superconductor being in the Fulde-Ferrell-Larkin-Ovchinnikov (FFLO) phase can be written as follows<sup>33</sup>

$$F' = \alpha(T)|\Psi'|^2 + \frac{\beta}{2}|\Psi'|^4 + \gamma(|\Pi_x\Psi'|^2 + |\Pi_y\Psi'|^2) \quad (A1) \\ + \delta(|\Pi_x^2\Psi'|^2 + |\Pi_y^2\Psi'|^2 + |\Pi_x\Pi_y\Psi'|^2 + |\Pi_y\Pi_x\Psi'|^2) \\ + \mu|\Psi'|^6,$$

where  $\Psi'$  is a complex superconducting order parameter and  $\Pi_{x,y} = \nabla_{x,y} - i(2e/\hbar c)A_{x,y}$ . As in Refs.<sup>16,19</sup> we neglect term with  $|\Psi'|^6$  (it allows us to decrease the number of free parameters) and define the signs of constants:  $\alpha, \gamma < 0$  and  $\beta, \delta > 0$  to have Fulde-Ferrell state as a ground one.

Ginzburg-Landau functional in the form similar to Eq. (A1) was derived from microscopic theory for clean thin superconducting film placed in parallel magnetic field<sup>34</sup>. We use here similar GL functional to model properties of superconductor/ferromagnet/normal metal trilayer being in Fulde-Ferrell state, where superconductor and ferromagnet are dirty metals with large resistivity. Therefore coefficients  $\alpha, \beta, \delta, \gamma$  should be considered only as a phenomenological parameters and  $\Psi'$  is a superconducting order parameter averaged over the thickness of SFN trilayer.

The dimensionless free energy  $F$  and order parameter  $\Psi$  are introduced as:  $F' = F_{GL}F = (\alpha^2/\beta)F$ ,  $\Psi' = \Psi_0\Psi = \sqrt{|\alpha|/\beta}\Psi$ , with defining of the characteristic length  $\xi_{GL} = \sqrt{|\gamma|/|\alpha|}$  and the dimensionless parameter  $\zeta = |\alpha|\delta/|\beta|^2$ . Varying  $\int F dS$  with respect to  $\Psi^*$ , we obtain the modified Ginzburg-Landau equation for the dimensionless order parameter:

$$\zeta\{\Pi_x^4 + \Pi_x^2\Pi_y^2 + \Pi_y^2\Pi_x^2 + \Pi_y^4\}\Psi \\ + \{\Pi_x^2 + \Pi_y^2\}\Psi + \Psi|\Psi|^2 - \Psi = 0. \quad (A2)$$

Equation (A2) has to be supplemented by the boundary conditions

$$\Pi\Psi|_n = 0, \quad \Pi^3\Psi|_n = 0. \quad (A3)$$

Our choice of boundary conditions provides vanishing of normal component of superconducting current  $j_s|_n$  and  $q|_n = (\nabla\phi - (2e/\hbar c)A)|_n$  on the boundary of superconducting square with vacuum. In ordinary Ginzburg-Landau model they vanish simultaneously if one chooses  $\Pi\Psi|_n = 0$  while in modified GL model one needs two conditions due to higher order of derivatives in Eq. (1). Vanishing of  $q|_n$  follows from the microscopic Usadel model for SFN trilayer, when superconducting current in each layer has to be equal to zero on boundary with vacuum. In framework of modified GL model one deals with averaged over the thickness current density  $j_s$ ,  $\lambda^{-2}$  and  $\Psi$ . In contrast to ordinary GL model it could be the situation when  $\lambda^{-2} = 0$  and, hence,  $j_s|_n \sim -\lambda^{-2}q|_n = 0$  while  $q|_n \neq 0$  which contradicts microscopic results for SFN trilayer. It is the reason why we use boundary condition  $\Pi\Psi|_n = 0$ . After making this choice vanishing of  $j_s|_n$  automatically leads to  $\Pi^3\Psi|_n = 0$ .

In numerical calculations we use relaxation method with adding of the time derivative  $\partial\Psi/\partial t$  in the right hand side of Eq. (A2) and looking for  $\Psi(x, y)$  which does not depend on time. In calculations we use two values of parameter  $\zeta = 0.5$  and 2. In both cases we obtain nearly the same results.

The transition from the homogenous to quasi 1D state is the second order phase transition as one increases  $L$ .

In framework of used model one can find analytically the critical size  $L_c$  when it occurs. By seeking the solution of Eq. (A2) in the following form:  $\Psi = (1 + |\delta\Psi|) \exp(i\phi)$  and assuming that  $|\delta\Psi| \ll 1$  and  $\nabla\phi \ll 1$  one can find that quasi 1D state may exist when  $L > L_c = \pi\sqrt{\zeta} = \pi/\sqrt{2}q_{FF}$  where  $q_{FF} = 1/\sqrt{2\zeta}$  is the optimal  $q$  which minimizes the free energy of FF bulk superconductor.

### Appendix B: Usadel model

To calculate superconducting properties of SFN disk we use 2D Usadel equation for anomalous  $F = \sin \Theta$  and normal  $G = \cos \Theta$  Green functions in polar coordinates

$$\hbar D \left( \frac{\partial^2 \Theta}{\partial z^2} + \frac{1}{r} \frac{d}{dr} r \frac{d\Theta}{dr} \right) - (2(\hbar\omega_n + iE_{ex}) + \hbar D q^2 \cos \Theta) \sin \Theta + 2\Delta \cos \Theta = 0, \quad (B1)$$

where  $D$  is a diffusion coefficient ( $D = D_S, D_F, D_N$  in superconducting, ferromagnet and normal layers, respectively),  $E_{ex} \neq 0$  is the exchange energy which is nonzero only in F layer,  $\hbar\omega_n = \pi k_B T(2n+1)$  is the Matsubara frequency,  $q = \nabla\phi + (2\pi/\Phi_0)A(r)$  ( $A$  is a tangential component of vector potential  $\mathbf{A} = (0, Hr/2, 0)$ ,  $\nabla\phi = N/r$ ,  $N$  is a vorticity),  $\Delta$  is a magnitude of superconducting order parameter which should be found in Usadel model with help of self-consistency equation

$$\Delta \ln \left( \frac{T}{T_{c0}} \right) + 2\pi k_B T \sum_{\omega_n \geq 0} \left( \frac{\Delta}{\hbar\omega_n} - \sin \Theta \right) = 0. \quad (B2)$$

We assume that in F and N layers  $\Delta = 0$  because of zero BCS coupling constant there.  $T_{c0}$  in Eq. (B2) is the critical temperature of single S layer. We consider disk with thickness  $d_S + d_F + d_N \ll \lambda$  and radius  $R \ll \lambda^2/(d_S + d_F + d_N)$ . Therefore we neglect corrections to  $A(r)$  which comes from superconducting currents.

Averaged over the thickness of the disc local  $\lambda^{-2}$  and superconducting current density are calculated as

$$\lambda^{-2} = \frac{16\pi^2 k_B T}{\hbar c^2 (d_S + d_F + d_N)} \times \int_0^{d_S + d_F + d_N} \frac{1}{\rho} \sum_{\omega_n \geq 0} \text{Re}(\sin^2 \Theta) dz \quad (B3)$$

$$j_s = -q \frac{c\Phi_0}{8\pi^2} \lambda^{-2}$$

with resistivity  $\rho = \rho_S, \rho_F, \rho_N$  in S, F and N layers, respectively.

At boundaries between different layers we use Kupriyanov-Lukichev boundary conditions<sup>35</sup> (for example  $D_S d\Theta/dz = D_F d\Theta/dz$  at  $z = d_S$ ) with fully transparent interfaces leading to continuity of  $\Theta$ . On the interface with vacuum we use  $d\Theta/dn = 0$ . Vanishing of normal component of superconducting current density (not

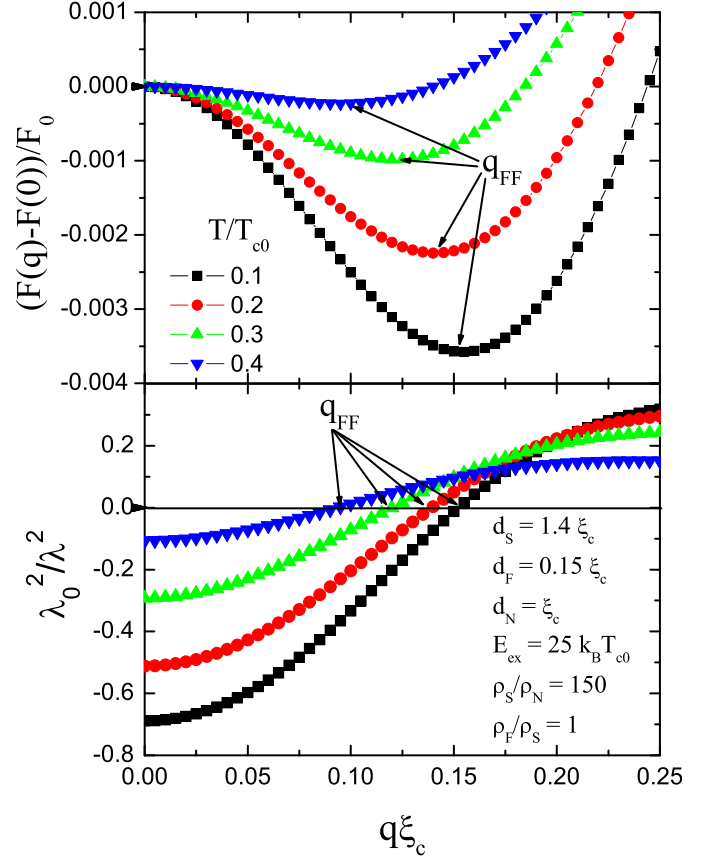


FIG. B.1: Dependence of the free energy (a) and averaged over the thickness of bulk SFN trilayer  $\lambda^{-2}$  (b) on  $q$ .  $\lambda^{-2} = 0$  in minimum of  $F(q)$ . Position of minimum shifts to smaller  $q$  with increasing temperature. For chosen parameters  $T_c = T_c^{FFLO}$ .

averaged over thickness) on the boundaries with vacuum leads to  $q|_n = 0$ . For considered homogenous and single/giant vortex states it is fulfilled automatically. In the center of the disk we use  $\Theta(r=0) = 0$  for vortex state and  $d\Theta/dr|_{r=0} = 0$  for homogenous one.

Equations (B1,B2) are solved numerically by using iteration procedure. For initial distribution  $\Delta(z, r)$  we solve Eq. (B1) for Matsubara frequencies ranging from  $n=0$  up to  $n=100$ . In numerical procedure we use Newton method combined with tridiagonal matrix algorithm. Found solution  $\Theta(z, r)$  is inserted to Eq. (B2) to find  $\Delta(z, r)$  and than iterations repeat until the relative change in  $\Delta(z, r)$  between two iterations is larger than  $10^{-8}$ . Length is normalized in units of  $\xi_c = (\hbar D_S/k_B T_{c0})^{1/2}$ ,  $\hbar\omega_n$ ,  $\Delta$  is in units of  $k_B T_{c0}$ , free energy (per unit of square) is normalized in units of  $F_0 = \pi N(0)(k_B T_{c0})^2 \xi_c$ , current density is in units of depairing current density of S-layer, magnetic field is in units of  $H_0 = \Phi_0/2\pi\xi_c^2$  and  $\lambda$  is in units of magnetic field

penetration depth in S layer  $\lambda_0$ . Step grid in  $z$  direction is  $dz = 0.01 - 0.05\xi_c$  (depending on the layer) and in radial direction  $dr = 0.1\xi_c$ . We check that results vary slightly with variation of  $dz, dr$  if they are small enough.

To decrease the number of free parameters we assume that the densities of states in S, F and N layers are the same and ratio of resistivities is equal to inverse ratio

of diffusion constants or mean path lengths  $\rho_S/\rho_N = D_N/D_S = \ell_N/\ell_S$ .

In Fig. B.1 we show dependence of free energy (it is calculated using Eq. (S5) in<sup>36</sup>) and  $\lambda^{-2}$  on  $q$  for bulk SFN trilayer. For chosen parameters  $T_c^{FFLO} = T_c \simeq 0.54T_{c0}$ . The minimum of  $F$  is reached at  $q = q_{FF}$  which depends on temperature.

- 
- \* Electronic address: plastovet26@gmail.com  
† Electronic address: vodolazov@ipmras.ru
- <sup>1</sup> F. S. Bergeret, A. F. Volkov, and K. B. Efetov, Josephson current in superconductor-ferromagnet structures with a nonhomogeneous magnetization, *Phys. Rev. B* **64**, 134506 (2001).
  - <sup>2</sup> Y. Asano, A. A. Golubov, Y.V. Fominov, and Y. Tanaka, Unconventional Surface Impedance of a Normal-Metal Film Covering a Spin-Triplet Superconductor Due to Odd-Frequency Cooper Pairs, *Phys. Rev. Lett.* **107**, 087001 (2011).
  - <sup>3</sup> T. Yokoyama, Y. Tanaka, and N. Nagaosa, Anomalous Meissner Effect in a Normal-Metal/Superconductor Junction with a Spin-Active Interface, *Phys. Rev. Lett.* **106**, 246601 (2011).
  - <sup>4</sup> H. Walter, W. Prusseit, R. Semerad, H. Kinder, W. Assmann, H. Huber, H. Burkhardt, D. Rainer, and J. A. Sauls, Low-Temperature Anomaly in the Penetration Depth of YBa<sub>2</sub>Cu<sub>3</sub>O<sub>7</sub> Films: Evidence for Andreev Bound States at Surfaces, *Phys. Rev. Lett.* **80**, 3598 (1998).
  - <sup>5</sup> Y. Asano, Y. V. Fominov, and Y. Tanaka, Consequences of bulk odd-frequency superconducting states for the classification of Cooper pairs, *Phys. Rev. B* **90**, 094512 (2014).
  - <sup>6</sup> M. Alidoust, K. Halterman, and J. Linder, Meissner effect probing of odd-frequency triplet pairing in superconducting spin valves, *Phys. Rev. B* **89**, 054508 (2014).
  - <sup>7</sup> Ya. V. Fominov, Y. Tanaka, Y. Asano, and M. Eschrig, Odd-frequency superconducting states with different types of Meissner response: Problem of coexistence, *Phys. Rev. B* **91**, 144514 (2015).
  - <sup>8</sup> A. Di Bernardo, Z. Salman, X. L. Wang, M. Amado, M. Egilmez, M. G. Flokstra, A. Suter, S. L. Lee, J. H. Zhao, T. Prokscha, E. Morenzoni, M. G. Blamire, J. Linder, and J.W. A. Robinson, Intrinsic Paramagnetic Meissner Effect Due to s-Wave Odd-Frequency Superconductivity, *Phys. Rev. X* **5**, 041021 (2015).
  - <sup>9</sup> F.K. Wilhelm, G.Schon, and A.D. Zaikin, Mesoscopic Superconducting-Normal Metal-Superconducting Transistor, *Phys. Rev. Lett.* **81**, 1682 (1998).
  - <sup>10</sup> A. M. Bobkov and I. V. Bobkova, Enhancing of the Critical Temperature of an In-Plane FFLO State in Heterostructures by the Orbital Effect of the Magnetic Field, *JETP Letters* **99**, 333 (2014).
  - <sup>11</sup> S.I. Suzuki and Y. Asano, Paramagnetic instability of small topological superconductors, *Phys. Rev. B* **89**, 184508 (2014).
  - <sup>12</sup> S. Mironov, A. Mel'nikov, and A. Buzdin, Vanishing Meissner effect as a Hallmark of in-Plane Fulde-Ferrell-Larkin-Ovchinnikov Instability in Superconductor/Ferromagnet Layered Systems, *Phys. Rev. Lett.* **109**, 237002 (2012).
  - <sup>13</sup> I. V. Bobkova and A. M. Bobkov, In-plane Fulde-Ferrel-Larkin-Ovchinnikov instability in a superconductor/normal metal bilayer system under nonequilibrium quasiparticle distribution, *Phys. Rev. B* **88**, 174502 (2013).
  - <sup>14</sup> S. V. Mironov, D. Yu. Vodolazov, Y. Yerin, A. V. Samokhvalov, A. S. Mel'nikov, and A. Buzdin, Temperature Controlled Fulde-Ferrell-Larkin-Ovchinnikov Instability in Superconductor-Ferromagnet Hybrids, *Phys. Rev. Lett.* **121**, 077002 (2018).
  - <sup>15</sup> P. M. Marychev and D. Yu. Vodolazov, Tuning the in-plane Fulde-Ferrell-Larkin-Ovchinnikov state in a superconductor/ferromagnet/normal-metal hybrid structure by current or magnetic field, *Phys. Rev. B* **98**, 214510 (2018).
  - <sup>16</sup> K. V. Samokhin and B. P. Truong, Fulde-Ferrell-Larkin-Ovchinnikov superconductors near a surface, *Phys. Rev. B* **99**, 014503 (2019).
  - <sup>17</sup> V. D. Plastovets and D. Y. Vodolazov, Dynamics of Domain Walls in a Fulde-Ferrell Superconductor, *JETP Lett.* **109**, 729 (2019).
  - <sup>18</sup> A. V. Samokhvalov, A. S. Mel'nikov, and A. I. Buzdin, Fulde-Ferrell-Larkin-Ovchinnikov states and quantum oscillations in mesoscopic superconductors and superfluid ultracold Fermi gases, *Phys. Rev. B* **82**, 174514 (2010).
  - <sup>19</sup> K. V. Samokhin, B. P. Truong, Current-carrying states in Fulde-Ferrell-Larkin-Ovchinnikov superconductors, *Phys. Rev. B* **96**, 214501 (2017).
  - <sup>20</sup> Supplemental material.
  - <sup>21</sup> B. J. Baelus, L. R. E. Cabral, and F. M. Peeters, Vortex shells in mesoscopic superconducting disks, *Phys. Rev. B* **69**, 064506 (2004).
  - <sup>22</sup> L. F. Chibotaru, A. Ceulemans, V. Bruyndoncx, and V. V. Moshchalkov, Symmetry-induced formation of antivortices in mesoscopic superconductors **408**, 833 (2000).
  - <sup>23</sup> V. R. Misko, V. M. Fomin, J.T. Devreese, and V.V. Moshchalkov, Stable Vortex-Antivortex Molecules in Mesoscopic Superconducting Triangles, *Phys. Rev. Lett.* **90**, 147003 (2003).
  - <sup>24</sup> A. A. Zyuzin and A. Yu. Zyuzin, Anomalous transition temperature oscillations in the Larkin-Ovchinnikov-Fulde-Ferrell state, *Phys. Rev. B* **79**, 174514 (2009).
  - <sup>25</sup> D. J. Thompson, M. S. M. Minhaj, L. E. Wenger, and J. T. Chen, Observation of Paramagnetic Meissner Effect in Niobium Disks, *Phys. Rev. Lett.* **75**, 529 (1995).
  - <sup>26</sup> A. E. Koshelev and A. I. Larkin, Paramagnetic moment in field-cooled superconducting plates: Paramagnetic Meissner effect, *Phys. Rev. B* **52**, 13559 (1995).
  - <sup>27</sup> A. K. Geim, S. V. Dubonos, J. G. S. Lok, M. Henini, and J. C. Maan, Paramagnetic Meissner effect in small superconductors, *Nature* **396**, 144 (1998).
  - <sup>28</sup> R. Panghotra, M. Timmermans, C. Xue, B. Raes, V. Moshchalkov, and J. Van de Vondel, Exploring the impact of core expansion on the vortex distribution in superconducting/normal-metal hybrid nanostructures,



- Phys. Rev. B **100**, 054519 (2019).
- <sup>29</sup> J. W. C. De Vries, Temperature-dependent resistivity measurements on polycrystalline SiO<sub>2</sub> covered thin gold films, *Thin Solid Films*, **150**, 201 (1987).
  - <sup>30</sup> B. L. T. Plourde, D. J. Van Harlingen, D. Yu. Vodolazov, R. Besseling, M. B. S. Hesselberth, and P. H. Kes, Influence of edge barriers on vortex dynamics in thin weak-pinning superconducting strips, *Phys. Rev. B*, **64**, 014503 (2001).
  - <sup>31</sup> T. Yamashita, A. Kawakami, and H. Terai, NbN-Based Ferromagnetic 0 and  $\pi$  Josephson Junctions, *Phys. Rev. Applied* **8**, 054028 (2017).
  - <sup>32</sup> V.S. Stolyarov, T. Cren, C. Brun, I. A. Golovchanskiy, O. V. Skryabina, D. I. Kasatonov, M. M. Khapaev, M.Yu. Kupriyanov, A. A. Golubov, D. Roditchev, Expansion of a superconducting vortex core into a diffusive metal, *Nature Communications*, **9**, 2277 (2018).
  - <sup>33</sup> A. Buzdin, Y. Matsuda and T. Shibauchi, FFLO state in thin superconducting films, *Europhys. Lett*, **80**, 67004 (2007).
  - <sup>34</sup> A.I. Buzdin, H. Kachkachi, Generalized Ginzburg-Landau theory for nonuniform FFLO superconductors, *Physics Letters A* **225**, 341 (1997).
  - <sup>35</sup> M. Yu. Kupriyanov and V. F. Lukichev, Influence of boundary transparency on the critical current of "dirty" SS'S structures, *Sov. Phys. JETP* **67**, 1163 (1988).
  - <sup>36</sup> M. Eltschka, B. Jack, M. Assig, O. V. Kondrashov, M. A. Skvortsov, M. Etzkorn, C. R. Ast, K. Kern, Superconducting scanning tunneling microscopy tips in a magnetic field: Geometry-controlled order of the phase transition, *Appl. Phys. Lett.* **107**, 122601 (2015).